Received: 23 November 2021 | Revised: 15 June 2022 | Accepted: 16 June 2022

DOI: 10.1002/ese3.1234

ORIGINAL ARTICLE

Metal-organic chemical vapor deposition of anatase titania on multiwalled carbon nanotubes for electrochemical capacitors

Edwin T. Mombeshora[1] | **Edigar Muchuweni**[1] | **Matthew L. Davies**[1,2] | **Vincent O. Nyamori**[1] | **Bice S. Martincigh**[1]

[1]School of Chemistry and Physics, University of KwaZulu-Natal, Durban, South Africa

[2]SPECIFIC IKC, Materials Science and Engineering, Faculty of Science and Engineering, Swansea University, Swansea, UK

Correspondence
Matthew L. Davies, SPECIFIC IKC, Materials Science and Engineering, Faculty of Science and Engineering, Swansea University, Swansea, UK.
Email: m.l.davies@swansea.ac.uk

Funding information

EPSRC Global Challenges Research Fund (GCRF) SUNRISE project, Grant/Award Number: EP/P032591/1; Inyuvesi Yakwazulu-Natali; Eskom Tertiary Education Support Programme; National Research Foundation of South Africa

Abstract

In practice, the capacitance from the electrochemical double layer formation on porous carbon-based electrodes is still below preferred values, limiting their use in electrochemical capacitors. The current drive is to innovate ways that generate additional capacitance in the electrochemical double layer capacitive nature of carbon nanomaterials towards both a high specific energy density (E_s) and power density (P_s). Herein we report the use of metal-organic chemical vapor deposition (MOCVD) to coat multiwalled carbon nanotubes (MWCNTs) with anatase titanium dioxide (TiO_2) to induce pseudocapacitive charge storage characteristics on a carbon-based electrode. The study shows that MWCNTs were coated in bundles, and targeted TiO_2 loadings were successfully attained, though the TiO_2 agglomerates also increased with TiO_2 wt.%. The 10 wt.% TiO_2 TiO_2-MWCNT material displayed the best capacitive behavior with associated specific discharge capacitance (C_d), E_s, and P_s values of 907 F kg^{-1}, 55.56 Wh kg^{-1}, and 2.78 W kg^{-1} at 0.1 A g^{-1}, respectively, due to the synergistic effect of the two components of the composite. Additionally, the integral capacitance (C_s) of the 20 wt.% TiO_2 material was enhanced more than 5000-fold relative to that of the 5 wt.% TiO_2 TiO_2-MWCNT composite at higher scan speeds of 100 and 200 mV s^{-1}. Electrochemical measurements further demonstrated the possible positive tuning of capacitive characteristics (charge/discharge rates, C_d and C_s) with TiO_2 wt.% control. The MOCVD synthesis method imparted the TiO_2-MWCNT composites with suitable traits that showed high potential in improving physicochemical processes favorable in electrical energy storage.

Edigar Muchuweni: On leave from Department of Engineering and Physics, Bindura University of Science Education, Private Bag 1020, Bindura, Zimbabwe.

KEYWORDS
carbon-based capacitors, electrochemical properties, energy storage, MWCNTs, titania-carbon composites

1 | INTRODUCTION

The continuous growth in the global population and advances in technology have triggered high demands for clean, sustainable, and renewable energy, and effective energy storage systems.[1–5] Electrical energy storage systems include batteries,[6] compressed air,[7] flywheels,[8] pumped hydro-energy,[9] conventional capacitors[10] and electrochemical capacitors (ECs).[11] ECs bridge the gap between batteries and conventional capacitors as emerging energy storage and power supply devices[2,12,13] due to environmental compatibility, lower costs, potentially higher energy and power densities, low-temperature dependencies, and better cyclabilities than conventional capacitors.[2,14–16] Hence, ECs have tremendous potential as static, passive, and portable energy storage devices, such as memory backup and hybrid/electric vehicle systems, that require rapid charge/discharge cycles.[17]

The energy storage capabilities of ECs are largely dependent on both the electrolyte and electrode materials.[12,13] Several materials, such as conducting polymers,[18] redox-based metal oxides[19,20] and carbon-based materials,[21,22] have been reported as suitable EC electrode materials. Of these, carbon-based materials offer attractive advantages that include lower cost, higher stability and conductivity, and better rate capability and reversibility than conventional redox-based metals/materials.[1,23] For instance, multiwalled carbon nanotubes (MWCNTs), due to their high surface area to volume ratio and facile surface functionalization that promotes polarizability, have been reported as suitable electrodes for charge storage devices.[21,24–27]

However, the specific capacitance of MWCNTs is far below the theoretical values of 400–500 $F\,g^{-1}$.[28,29] The current drawbacks of carbon-based materials include their low capacitive characteristics, partly because of poor polarizability and wettability associated with the electrode surfaces, which limit the available surfaces for energy storage.[1,30] To improve on the weaknesses of carbon-based materials, the synthesis of composite materials can engineer interconnected structures that have ample potential to shorten the charge diffusion path length of carbon materials.

In particular, composites of MWCNTs with metal oxides, such as MnO_2, NiO, Fe_2O_3, and TiO_2, have been used to improve the specific energy density and integral specific capacitance (C_s) linked to MWCNTs.[23,31] The use of titanium dioxide (TiO_2) in several applications has been motivated by its semiconductor properties, long-term chemical stability, and availability of surfaces for chemical processes.[2] TiO_2 is known for its high rate of agglomeration and wide band gap (~3.2eV), which have limited its applications. For instance, the wide band gap limits effective utilization of visible light and causes rapid electron/hole recombination, thereby lowering the photocatalytic activity[32,33] and power conversion efficiency of solar cells.[34] Effective charge separation (electron transport) in TiO_2 for catalytic applications has been achieved through composite synthesis with carbonaceous materials and creating maximum contact between components, although sample homogeneity is a common shortcoming.[33,35,36] Similarly, a wide band gap and agglomeration effects have led to a lower theoretical capacitance and high resistivity (strong internal resistance).[1,2] Despite the shortcomings, TiO_2 can be used as a coating material since it can tune the physicochemical properties of MWCNTs, such as hydrophilicity of the electro-active surfaces, and introduce pseudocapacitive effects on MWCNTs due to its variable oxidation state.[13,21,37] Also, electron/hole recombination of TiO_2 is minimal in composites with MWCNTs.[34,38] In addition, all the phases of TiO_2, namely, rutile (most thermodynamically stable), brookite, and anatase (most kinetically stable, low sintering temperature), have been studied in EC applications and the studies show that capacitance depends more on the structural features, such as sizes, rather than phases.[39–41] Hence, due to low sintering temperature requirements, the anatase phase may be preferable.

Studies on TiO_2-MWCNT composites for EC applications have been previously reported. For example, Hsieh et al.[14] synthesized a TiO_2-MWCNT composite for EC applications in an H_2SO_4 electrolyte from titanium isopropoxide through a wet impregnation method followed by heating. They concluded that a high TiO_2 wt.% blocks the electrochemical double layer capacitance (EDLC) contributions from MWCNTs. The same authors also reported a wet impregnation synthesis method, followed by microwave deposition of TiO_2 from tetrabutyl titanate onto MWCNTs, which improved C_s by 1.37-fold in H_2SO_4 electrolyte.[13] Kim et al.[30] synthesized TiO_2-MWCNT composites by a sol-gel method from titanium isopropoxide that enhanced the C_s 1.68-fold also in the H_2SO_4 electrolyte. Krishnaveni and Anandan[42]

also reported unzipped MWCNTs in TiO_2-MWCNT through an ultrasound-assisted method for EC applications in Na_2SO_4 that achieved an 8.54-fold enhancement.

The synthetic method of a material is crucial in developing suitable alternatives to conventional electrode materials.[42] This is because each method imparts unique merits/demerits to the physicochemical properties of the material, such as substantial isolated TiO_2 agglomerates common in composites synthesized by means of the sol-gel method.[36,43] Hence, the current work reports the use of a metal-organic chemical vapor deposition (MOCVD) method to synthesize TiO_2-MWCNT composites from a titanium(IV) methoxide precursor for EC applications. To the best of our knowledge, no such report exists in the literature. The study also aims to increase the charge/discharge rates of MWCNTs and facilitate the pseudocapacitive characteristics and the electrochemical double layer behavior of pristine MWCNTs by the addition of TiO_2. The effect of the morphology of the MWCNTs coated with anatase TiO_2 in terms of associated physicochemical properties and EC applications was also investigated. Hence, the current study investigated the MOCVD synthesis of TiO_2-MWCNT, culminating in a unique morphology and charge storage capabilities.

2 | EXPERIMENTAL SECTION

2.1 | Materials and reagents

MWCNTs (outer diameter: 8–15 nm, length: 10– 50 μm, ash: <1.5 wt.%, SSA: >233 $m^2 g^{-1}$, EC: >10^{-2} S cm^{-1}, SKU number 030102, ~95 wt.%) were purchased from Cheaptubes.com. Concentrated sulfuric acid (AAR, 98%–100%) and hydrochloric acid (≥32%) were procured from SSM Instruments, while nitric acid (≥69%) and both titanium (IV) methoxide (95%) and Nafion (20 wt.% solutions in lower aliphatic alcohols/H_2O containing 34% water) were from Sigma-Aldrich. Na_2SO_4 (97%) for the electrolyte was purchased from Merck.

2.2 | Composite synthesis

A mass of 1 g of MWCNTs was acid-treated in 3:1 (v/v) HNO_3/HCl, respectively, by means of an ultrasonic water bath for 4 h. The acid-treated MWCNTs were then washed with double-distilled water until the filtrate was neutral in pH and, thereafter, dried at 120°C in an oven (Scientific Economy Series, Model 220-224). Subsequently, a predetermined mass of acid-treated MWCNTs was mechanically mixed with a known mass of titanium(IV) methoxide using a pestle and mortar to synthesize composites (5, 10, and 20 wt.% TiO_2). The mixture was loaded into an MOCVD reactor, reported elsewhere,[34] and the reactor was inserted in a horizontally aligned tubular furnace (Scientific Economy Series, Model 220-224). Initially, during the synthesis, the MOCVD reactor, connected to a vacuum pump, was evacuated to an absolute pressure of 0.01 mbar, measured with a Thyracont VD84/1 Pirani vacuum gauge. Thereafter, the furnace temperature was increased to 100°C at a rate of 2°C min^{-1} and then held constant for 60 min. The vacuum pump was turned off, and the valve connector to the reactor was also closed before another temperature increase to 400°C at 2°C min^{-1}. The temperature was held constant at 400°C for 60 min before cooling to room temperature.

2.3 | Physicochemical characterization

The TiO_2-MWCNT nanocomposites were characterized by various techniques. Transmission electron microscopy (TEM) and scanning electron microscopy (SEM) analyses were carried out using JEOL TEM 1010 and JEOL JSM 6100 electron microscopies, respectively. X-ray energy-dispersive (EDX) spectra were acquired with a Bruker X-ray spectrometer attached to the JEOL JSM 6100 SEM instrument. For textural analyses, the samples were degassed at 90°C for 60 min and thereafter at 160°C overnight, and the actual analyses were performed with a Micromeritics TriStar 3020 (V1.03) surface area and porosity analyzer at 77 K with N_2 gas as the adsorbate. For Fourier transform infrared spectroscopy (FTIR) analysis, spectra were acquired with a PerkinElmer FTIR spectrometer (Spectrum RX1, version 5.3), and samples mixed with KBr at a known ratio were pelletized in a 25-ton ring press (00-25 model, Research Industrial Company, England). The Raman analysis was performed at 514 nm with 50% laser power and a 10 s exposure time using a Renishaw inVia Raman microscope. The Raman bands were fitted to a Gaussian function. Powder X-ray diffraction (XRD) analysis was done by means of a D8 Advance diffractometer (BRUKER AXS, Germany) with PSD Vantec-1 detectors. Measurements were done with a θ-θ scan in locked coupled mode and Cu-Kα radiation ($\lambda = 1.5406$ Å). The International Centre for Diffraction Data database for 1998 and EVA software (BRUKER) were used for peak assignment. Thermal stability analysis was carried out with a TA Instruments Q series™ Thermal Analyzer DSC/TGA (Q600) coupled with TA instruments Universal Analysis 2000 software for data acquisition and thermogram analysis.

2.4 | Electrochemical measurements

Electrochemical characterizations were performed by galvanostatic charge/discharge (GCD), electrochemical impedance spectroscopy (EIS), and cyclic voltammetry (CV) techniques. The fabrication of a CV working electrode involved mixing 95 wt.% composites with 5 wt.% Nafion as a binder (5 wt.% Nafion) and thereafter casting onto a 3 mm diameter glassy carbon electrode that had previously been cleaned and polished. The working electrode was dried under room temperature conditions. A Metrohm 797 VA Computrace electrochemical workstation (Metrohm, Switzerland) comprising of a three-electrode system (Pt counter and Ag/AgCl reference electrodes), 1 M Na_2SO_4 electrolyte (typically degassed with nitrogen for five min before analysis), a scan range of 0–0.8 V, and scan speeds of 10, 25, 50, 100 and 200 mV s^{-1}, were used for CV. The C_s from the CV curve was calculated by using the following equation:[17,23,26]

$$C_S = \frac{1}{2}\frac{\int idV}{msV}, \tag{1}$$

where i (A), m (g), s (V s^{-1}), and ΔV (V) are the current, active material mass, scan speed, and voltage window, respectively. Integration was done by use of the Lorentzian function.

EIS and GCD were carried out using a Princeton Applied Research VersaSTAT 3F, model-500, potentiostat/galvanostat with a three-electrode system (working electrode with 95 wt.% composite and 5 wt.% Nafion binder cast onto a glassy carbon, Pt counter, and Ag/AgCl reference electrodes). The VersaStudio software (version 2.60.6.0) was used for data acquisition. For EIS, the frequency range was 100,000—1 Hz, and the AC voltage used was 5 mV. A current density of 0.1 A g^{-1} was used in GCD analysis for the determination of specific discharge capacitance (C_d), specific energy density (E_s), and power density (P_s) of the TiO_2-MWCNT composites. Equation (2) can be used to determine C_d in F kg^{-1} from the GCD plots.[1,2]

$$C_d = \frac{i_d \Delta t}{m\Delta V}, \tag{2}$$

where i_d (A), Δt (s), ΔV (V), and m (kg) are the discharge current, discharge time, potential window on the time-voltage graph (GCD curve), and the active material mass, respectively. Equation (2) can be simplified to Equation (3); hence, for the determination of C_d, Equation (3) was used.

$$C_d = \frac{i_d}{mg}, \tag{3}$$

where g is the gradient determined from the GCD curve as reported elsewhere.[15,17] E_s (Whkg^{-1}) and P_s (W kg^{-1}) were calculated by using Equations (4) and (5), respectively[23]:

$$E_s = \frac{1}{2}C_s \Delta V^2, \tag{4}$$

$$P_s = \frac{E}{\Delta t}. \tag{5}$$

3 | RESULTS AND DISCUSSION

In this study, composites of MWCNTs coated with three different amounts of TiO_2, namely, 5, 10, and 20 wt.%, were prepared by an MOCVD method. The physicochemical and electrochemical properties of the synthesized materials were fully characterized to determine the unique characteristics imparted by the synthetic method used, especially as regards the enhancement of properties required for their use in EC devices.

Scanning electron microscopy provided evidence that the degree of coating on the tubular MWCNTs increased with increasing TiO_2 wt.% (Figure 1A,C,E,G). The decrease in the visibility of the inner cavity of MWCNTs in the TEM micrographs corroborated with the increase in TiO_2 coating determined by means of SEM (Figure 1D–F and Supporting Information: Figure S1). In the case of the 5 wt.% material, the coating of the tubes was not uniform, with some bare parts visible in TEM micrographs, SEM images and superimposed EDX (Figure 1C,D and Supporting Information: Figure S2). This effect could have been influenced by the location of oxygen-containing groups in which these sites are preferred initially, but at higher TiO_2 loadings, this effect is minimal. Contrary to other synthetic methods, such as sol-gel[34] and wet impregnation,[44] which coated MWCNTs individually, MOCVD coated bundles of MWCNTs together (highlighted by circles in Figure 1). This possibly arose because the MOCVD method involved the vaporization of the titanium methoxide precursor under vacuum in facilitating the deposition of TiO_2 on the MWCNTs, and the method had no control over the number of tubes that were coated together, despite the mechanical mixing of the starting materials with a pestle and mortar before loading into the reactor. Hence, some MWCNTs were coated with TiO_2 into bundles at 20 wt.% TiO_2 (circled in Figure 1G-H). Unlike the report by Hsieh et al.,[14] which involved the synthesis

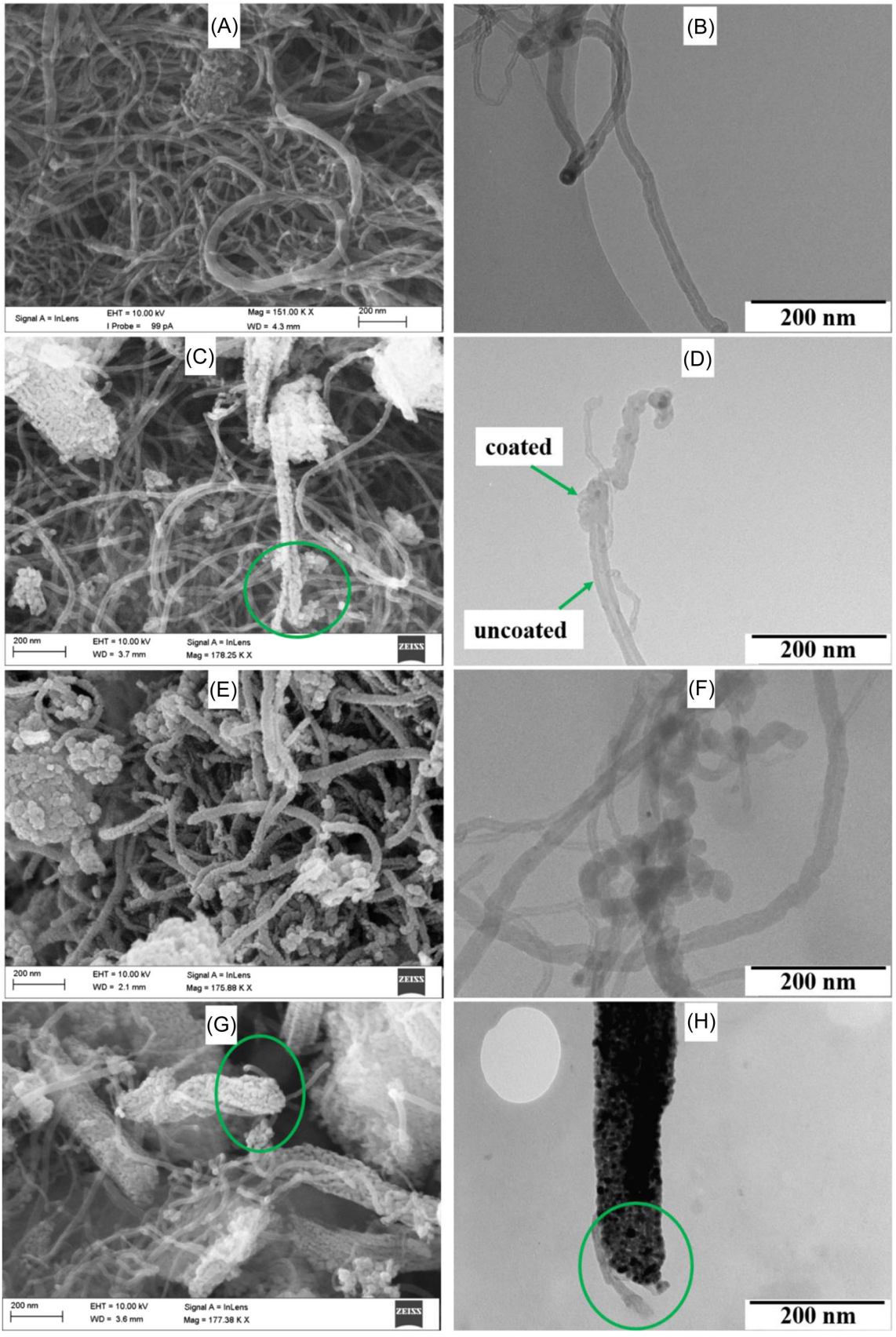

FIGURE 1 SEM and TEM images respectively of (A, B) MWCNTs and TiO_2-MWCNT composites coated with (C, D) 5 wt.%, (E, F) 10 wt.%, and (G, H) 20 wt.% TiO_2. SEM, scanning electron microscopy. TEM, transmission electron microscopy.

of TiO_2-MWCNT through a chemical-wet impregnation method, isolated aggregates of TiO_2 were not observed in the current work at higher TiO_2 wt.%.

Energy-dispersive X-ray (EDX) spectroscopy was used for qualitative purposes, and it confirmed the incorporation of TiO_2 and MWCNTs in composites (Supporting Information: Figure S2). An increase in the Ti signal supported the changes in wt.% in the composites, and SEM morphologies agreed with the changes in the elemental distribution in the superimposed EDX spectra (Supporting Information: Figure S2). The superimposed EDX spectra for the composites support the coating of bundles of MWCNTs with TiO_2 with no visible isolated TiO_2 aggregates (Supporting Information: Figure S2).

The Brunauer–Emmett–Teller (BET) surface areas and pore volumes of the three composite materials decreased as the TiO_2 wt.% increased (Table 1). This was ascribed to the bundling of the coated MWCNTs. A similar decline in BET surface areas was also reported for composites synthesized by the sol-gel method.[30] Despite this clear inversely proportional effect as regards porosity and BET surface area, the pore sizes were smallest for the 10 wt.% TiO_2 material. This implies that a higher TiO_2 wt.% blocked the MWCNT pores for nitrogen sorption, which could be due to the increased agglomerates. All three composites showed a type IV isotherm with an H3 hysteresis loop, indicative of mesoporous materials (Supporting Information: Figure S3), and hence, they are suitable for EC applications.

TABLE 1 Textural characteristics of TiO_2-MWCNT nanocomposites

TiO_2 wt.%	BET surface ($m^2\ g^{-1}$)	Pore volume ($cm^3\ g^{-1}$)	Pore size (nm)
0	143	0.50	13.98
5	139	0.84	23.84
10	130	0.68	20.24
20	126	0.63	22.34

Abbreviations: BET, Brunauer–Emmett–Teller; MWCNT, multiwalled carbon nanotube.

FTIR spectral analysis showed the presence of a Ti–O–OC bond at 1100 cm^{-1}, which indicates that some TiO_2 molecules were covalently attached to the MWCNTs through the oxygen-containing moieties (Figure 2). During the first step of the MOCVD synthesis, the temperature was increased to 100°C and the valve was opened, thereby eliminating water vapor from the reagents. The peak at 3400 cm^{-1} was ascribed to the hydroxyl groups from atmospheric moisture. The peaks at 2300, 1600, and 600 cm^{-1} were attributed to H-bonding effects from oxygen-containing moieties, C=C in the MWCNTs framework, and the presence of the anatase phase of TiO_2, respectively (Figure 2).[42]

Consistent with FTIR spectrophotometry, Raman spectroscopic bond vibrational analysis showed the presence of anatase TiO_2 through the observed peaks at ca. 154 cm^{-1} (E_g), 399 cm^{-1} (B_{1g}) and 639 cm^{-1} (E_g), and similar peaks were detected for the TiO_2-MWCNT composites (Figure 3 and Supporting Information: Figure S4).[1,35,42,45–47] Also, the small peak at 800 cm^{-1} was ascribed to the Ti–O–H covalent bond vibration,[45] which corroborated with the FTIR data (Figures 3 and 4). The Ti–O–H covalent bond is an indication that TiO_2 also interacted with MWCNTs via OH functionalities on the tube walls. The Raman bands at 1350 and 1600 cm^{-1} were assigned to the structural defects of the C-C framework (D-band) and C-C tangential in-plane stretching (G-band), respectively.[1,42]

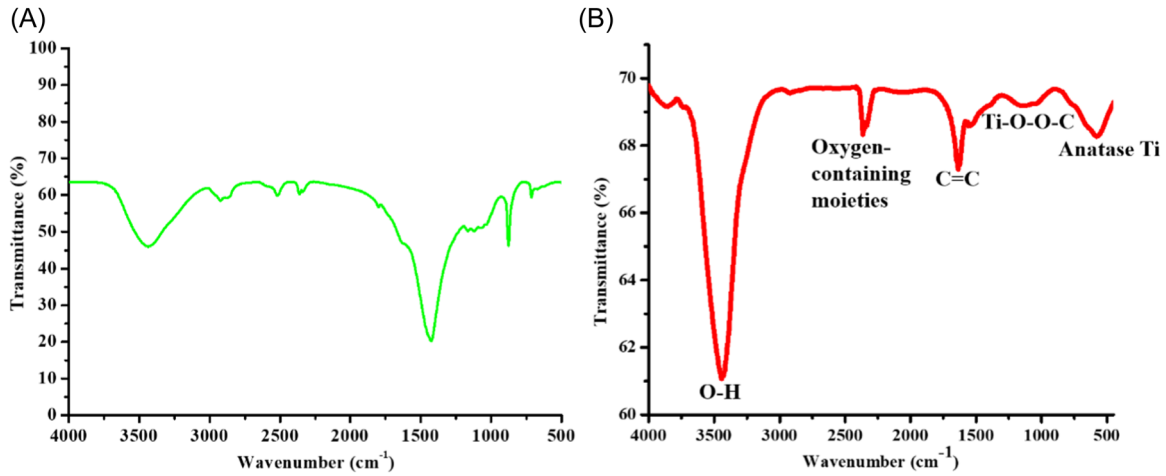

FIGURE 2 (A) FTIR spectrum of MWCNTs, and (B) representative FTIR spectrum for the nanocomposites, acquired as KBr discs. FTIR, Fourier transform infrared spectroscopy; MWCNT, multiwalled carbon nanotube.

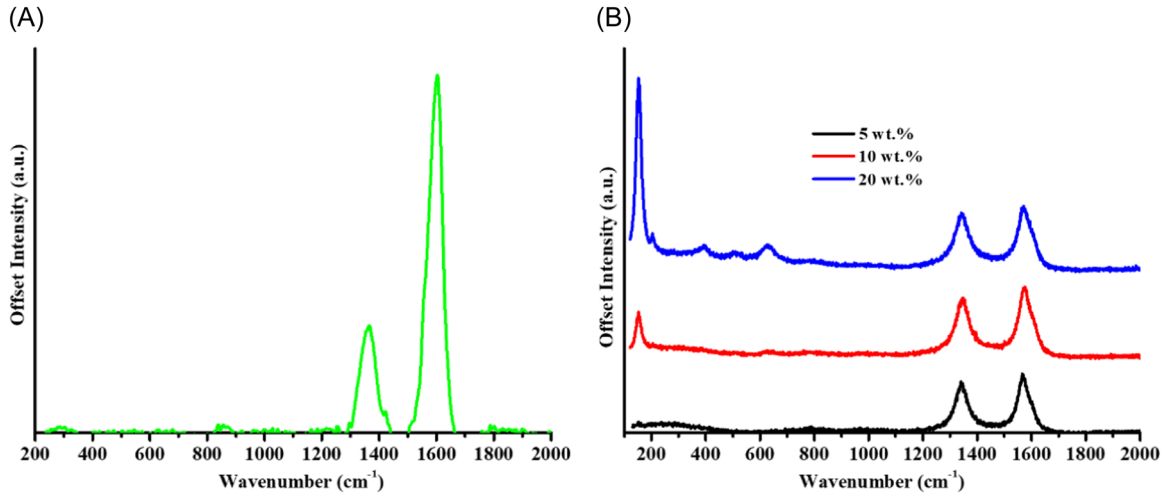

FIGURE 3 Raman spectra for (A) MWCNTs and (B) the TiO_2-MWCNT composites at different TiO_2 wt.% as indicated in the inset. MWCNT, multiwalled carbon nanotube.

FIGURE 4 Powder X-ray diffractograms for TiO_2-MWCNT nanocomposites synthesized with 5, 10, and 20 wt.% TiO_2. MWCNT, multiwalled carbon nanotube.

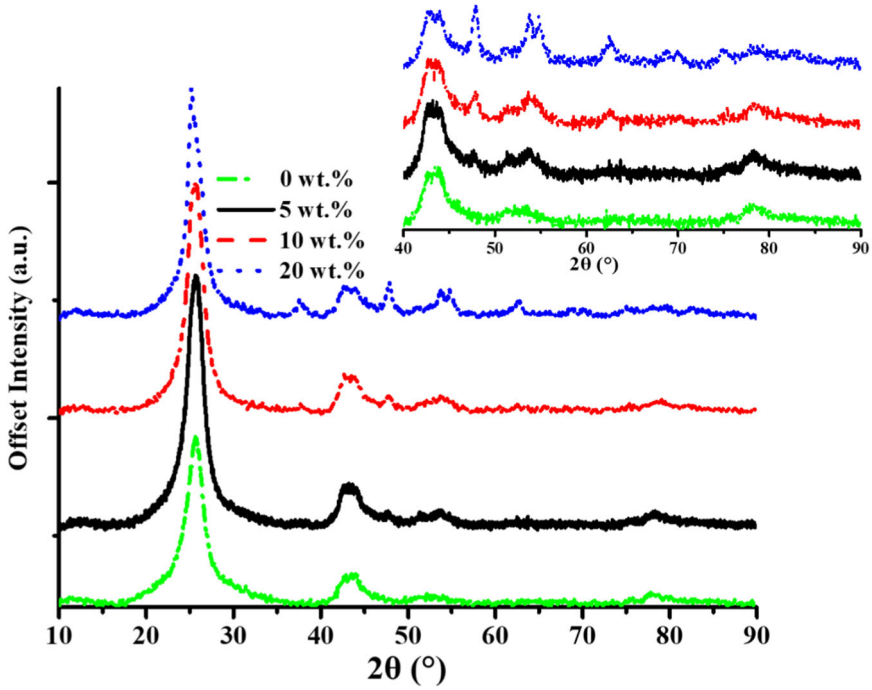

The higher TiO_2 wt.% led to a wider full width at half maximum (FWHM) of the G-band, suggesting that either TiO_2 sits on the MWCNT defects or the covalent link through oxygen moieties reduces the defect intensity. A similar trend was observed in the defect intensity (I_D/I_G) calculated as the ratio of the area under the D-band to that under the G-band (Table 2 and Supporting Information: Figure S4). Despite all composites displaying higher defect intensities than pristine MWCNTs, the Raman data probably suggests that the TiO_2 wt.% investigated were not excessively straining (less defective) on the carbon backbone. This is consistent with

TABLE 2 Raman data for the nanocomposites synthesized using the MOCVD approach

	D band		G band		
TiO_2 (wt.%)	Position (cm^{-1})	FWHM	Position (cm^{-1})	FWHM	I_D/I_G
0	1349	58	1602	42	0.59
5	1343	59	1571	58	0.93
10	1346	66	1576	63	0.91
20	1345	66	1574	67	0.87

Abbreviations: FWHM, full width at half maximum; MOCVD, metal-organic chemical vapor deposition.

previous reports in that the amount of TiO_2 may not necessarily affect the defect intensity but an increase in the amount of TiO_2 may shift the G-band position to lower energies (Table 2).[48–50] In addition, the shift for the ill-organized graphite (D-band) indicates that MWCNTs are adsorbed and bound to the TiO_2 surfaces as deduced by means of FTIR spectrophotometry (Figure 2).[49,51]

The crystallinity and phase of TiO_2 present in the composites were evaluated by powder XRD. The X-ray diffractograms exhibited peaks at 2θ values of 42°, 78°, 25°, 36°, 48°, 54°, 63°, and 70°. These were assigned to the reflection from the (100) and (222) planes of MWCNTs, TiO_2 (101) plane/MWCNTs (002) plane overlap, and (004), (200), (105), (204), (220) and (215) planes of anatase TiO_2, respectively (Figure 4).[14,23,30,44,52] Additionally, the relative intensity of peaks due to the reflections of the (200), (105), (204), and (220) anatase TiO_2 planes (insert in Figure 4) increased in proportion to the wt.% of TiO_2 providing further evidence to support the composition of the composites. This suggests that a TiO_2 deposition temperature of 400°C in the final MOCVD synthesis step agrees with the reported stability of the anatase phase of TiO_2 at temperatures lower than 500°C.[2,21] The presence of characteristic peaks from both composite components indicates that the nanocomposites were effectively synthesized via the MOCVD method. The sharp peaks observed for all samples indicate the presence of TiO_2 crystallites in the composites (Figure 4).

Thermal analysis of the materials in an atmosphere of air confirmed the TiO_2 wt.% loadings on the MWCNTs. The residual mass beyond 650°C was ascribed to the TiO_2 component, as metal oxides are thermally stable below 1000°C under air (Figure 5A). The residual mass was proportional to the TiO_2 wt.% and was slightly more than the target TiO_2 loadings. Despite purification in acid, the slight variation was due to the residual Fe from the pristine MWCNT synthesis; hence, this suggests a successful TiO_2 loading. The TiO_2 quantification, using TGA, of similar precision to the preparative values has been previously reported.[2,13] The wt.% of TiO_2 exhibited a negligible effect on the thermal stability of C=C bonds in the MWCNTs framework (Figure 5). All the materials decomposed at approximately the same temperature of 600°C. The shoulder on the derivative wt.% curve of 5 wt.% TiO_2 TiO_2-MWCNT is attributed to uncoated MWCNTs (Figure 5B).

After confirming that the composite materials had been successfully synthesized by the MOCVD method, they were characterized electrochemically for their possible application in charge storage devices. Quasi-rectangular CV curves were observed at low scan speeds, but these deteriorated with an increase in scan speed (Figure 6A–E and Supporting Information: Figure S5 showing that the voltammograms of 5 wt.% TiO_2 material are present in Figure 6B–E but not visible due to Figure 6 scale). At low scan speeds, voltammograms also display that the composites had better quasi-rectangular CV shape and were similar to bare MWCNTs, but at high scan speeds, higher wt.% composites are better than bare MWCNTs and the 5 wt.% composites (Figure 6). This infers that at low scan speed, charge reversal was faster and exhibited charge storage mostly via the EDLC mechanism.[1,15] The elliptical shape of the CV curve (deviation from rectangular shape) at higher scan speeds can be attributed to the high pore resistance of the composites, poor wettability, and minimal contributions of electrolyte ions to charge transfer processes at the material interfaces.[53] The increase in current response as scan speed was raised was attributed to the

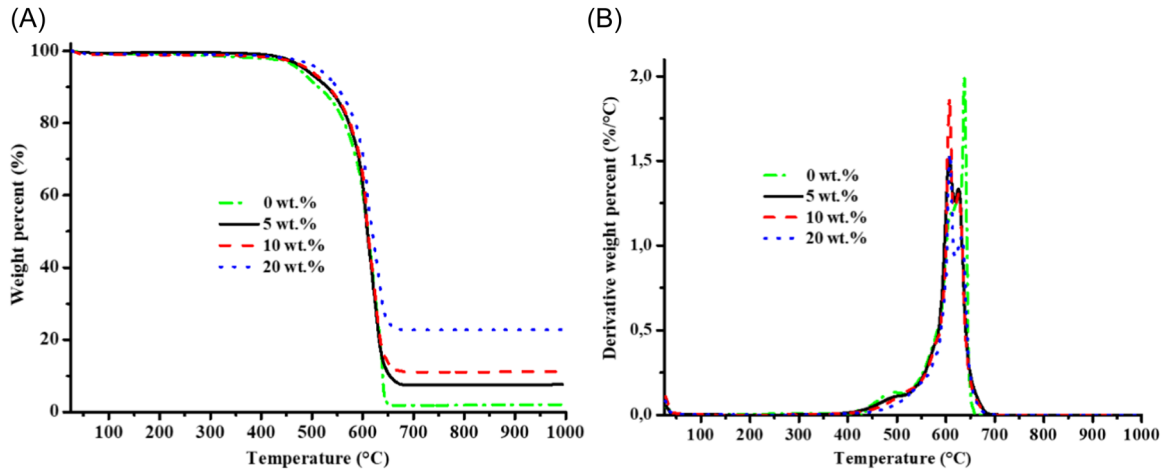

FIGURE 5 Thermal stability of the TiO_2-MWCNT nanocomposites determined in an atmosphere of air: (A) thermograms and (B) derivative thermograms. MWCNT, multiwalled carbon nanotube.

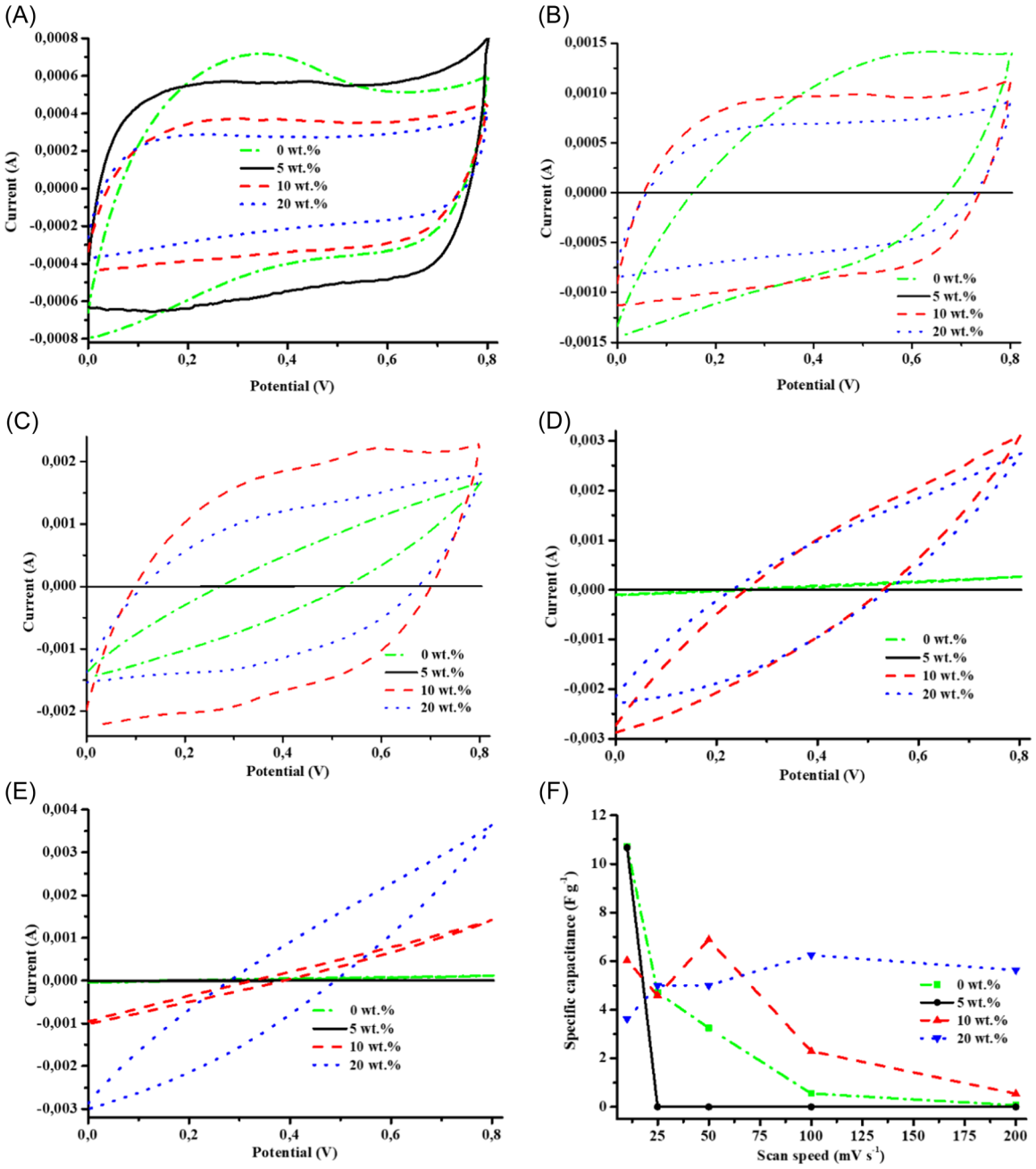

FIGURE 6 Effect of TiO_2 wt.% in TiO_2-MWCNT nanocomposites on electrochemical properties determined by cyclic voltammetry at scan speeds of (A) 10, (B) 25, (C) 50, (D) 100, (E) 200 mV s^{-1}, and (F) variation of integral specific capacitance with scan speed. MWCNT, multiwalled carbon nanotube.

corresponding decrease in diffusion layer size due to the better rate capability of the composites.[23,54] At 10 mV s^{-1}, the 5 and 20 wt.% TiO_2 materials displayed the best and worst capacitive qualities, respectively. A probable reason for the 5 wt.% TiO_2 composites displaying the best EDLC quality at 10 mV s^{-1} (Figure 6A) is that the BET surface area reflected the available electrochemically active surfaces; hence, since the 5 wt.% TiO_2 material exhibited the largest surface area, this enhanced the surfaces available for the formation of the electrochemical double layer (Table 1). This trait is also supported by the BET surface area and capacitive quality of MWCNTs (0 wt.% TiO_2) relative to the 10 and 20 wt.% TiO_2 materials (Figure 6A and Table 1). The positive effect of composite synthesis was displayed by the severe deterioration of EDLC quality and capacitance of pristine MWCNTs with the increase in scan speed (Figure 6A–F).

Additionally, while the TiO_2-MWCNT composite of 5 wt.% TiO_2 deteriorated severely, worse than MWCNTs, in terms of EDLC characteristics at scan rates of 25 and

50 mV s^{-1}, the optimum TiO_2 wt.% was 10 (Figure 6B,C). This could be because the 10 wt.% material had a more homogeneous coating with a thin and conformal TiO_2 deposition on individual CNTs, thus, maximizing the wettability and electrochemically active surface area even though it had the smallest pore sizes (Figure 1 and Table 1). Beyond 50 mV s^{-1}, despite the severe EDLC character decline due to insufficient time for electrolyte ions to penetrate inner pores, the 20 wt.% TiO_2 composites exhibited the best EDLC behavior. Similarly, the highest enclosed area in the CV loop, indicating the highest calculated C_s, at low and high scan speeds, was obtained from low and high wt.% of TiO_2 in TiO_2-MWCNT, respectively (Figure 6E). As pristine carbon-based materials portray well-observed EDLC mechanisms,[10,12,55] a more plausible explanation of the observed traits is that at low scan speeds, the charge storage contributions, mostly from MWCNTs, are not influenced by the wettability effect of TiO_2.[13] Also, at 10 mV s^{-1}, enough time was afforded for electrolyte ion penetration into the pores, and therefore the surface area effect was more dominant in influencing C_s (Table 1 and Figure 6F). However, the C_s was independent of BET surface area at higher scan rates. Unlike the usual C_s decline of metal oxide-based electrodes as the scan rate is increased because of associated low conductivities,[2] the C_s of the 20 wt.% TiO_2 TiO_2-MWCNT increased. This could be because surface-controlled reactions induced by TiO_2 in electrodes increased as scan speed was raised.[56] Additionally, at 10 mV s^{-1}, the current work is in agreement with the work reported by Kim et al.[30] (involving 4, 6, 17, and 33 wt.% of TiO_2) in that C_s declines with an increase in TiO_2 wt.% in TiO_2-MWCNT (Figure 6F). However, the current work varied from this trend at higher scan rates (100 and 200 mV s^{-1}) in that the 20 wt.% TiO_2 TiO_2-MWCNT material displayed a 5000-fold improvement of C_s relative to that of 5 wt.% (Figure 6F and Supporting Information: Table S1). The rationale behind the raised capacitive characteristics of the TiO_2-MWCNT nanocomposites at both higher TiO_2 wt.% and scan speeds is the synergistic effects from morphological variations, induced pseudo mechanism,[13,14] and enhanced hydrophilicity from TiO_2.[2] Hydrophilicity from TiO_2 enhances the surface available for the formation of the electrochemical double layer.[13] Hence, this study highlights the effect of both the Na_2SO_4 electrolyte and the TiO_2 wt.% in the TiO_2-MWCNT composites on both the charge storage mechanism and capacitance through synergistic effects of active sites and conductivity factors introduced by the use of heat during the MOCVD synthesis method.

Similar to the deductions arrived at from CV, the 10 wt.% TiO_2 TiO_2-MWCNT composite relatively displayed the most symmetrical GCD voltage-time profile supporting the highest capacitive character with unsurpassed electrochemical reversibility during the charge/discharge cycles than the rest of the composites (Supporting Information: Figures S6 and S7). The discharge times at 5, 10, and 20 wt.% TiO_2 were 10, 20, and 1 s, respectively. The longest discharge time was attributed to the optimum synergistic capacitive capabilities from both the EDLC and the pseudocapacitance contributions from the 90 wt.% MWCNTs:10 wt.% TiO_2, in the TiO_2-MWCNT composite, respectively. Even though the E_s was also optimum at 10 wt.% TiO_2, the 20 wt.% TiO_2 TiO_2-MWCNT composite exhibited a slightly smaller value, and this could be attributed to the similar defect intensity and pore volumes of the two composites (Tables 1–3), which affects the electrolyte ion movement (carrying the charge) and penetration into the electrode material, respectively. Additionally, the power density increased significantly as the TiO_2 wt.% was raised (Table 3), which corroborated with the higher C_s at high scan rates (Figure 6F). The E_s and P_s values in the current work are higher than those reported for TiO_2 carbon-based composite materials.[2] This also agrees with earlier reports in that materials with low energy density (usually poor capacitive capabilities from short discharge time) are typically associated with higher power densities.[57,58] The reasons for these traits are the fast charge/discharge attributes induced by the pseudocapacitive features at higher TiO_2 wt.%.[57,59,60]

On the one hand, EIS measurements showed that the semi-circle in the higher frequency region of the 20 wt.% TiO_2 nanocomposite was larger than that of the 5 wt.% TiO_2 TiO_2-MWCNT nanocomposite, and this infers a higher charge transfer resistance (R_{CT}) at 20 wt.% TiO_2 (Figure 7).[1] The higher R_{CT} of almost 110 Ω for 20 wt.% TiO_2 could be rationalized by the large number of TiO_2 agglomerates that disrupted the surface morphology interconnectivity, thereby causing poor conductivity (Figure 7). This could be further ascribed to the MOCVD bundling effect on MWCNTs because of the lack of mixing/stirring during composite synthesis. Additionally, the increase in R_{CT} at high TiO_2 wt.% agrees with the study results on atomic layer deposition of rutile TiO_2 on vertically aligned MWCNTs.[21] Hence, this infers that the traits in the current

TABLE 3 Calculated specific discharge capacitance (C_d), energy (E_s), and power (P_s)

TiO_2 wt.%	C_d (F kg^{-1})	E_s (Wh kg^{-1})	P_s (W kg^{-1})
5	0.04	0.01	0.01
10	907.03	55.56	2.78
20	95.74	47.87	47.87

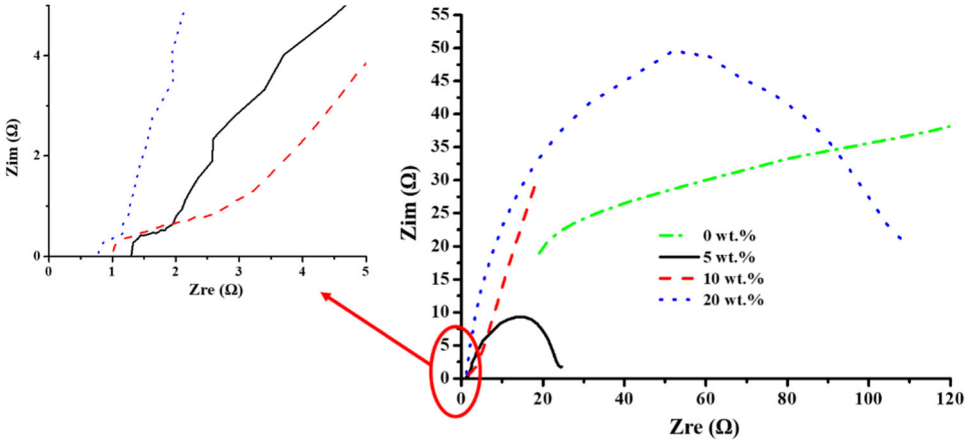

FIGURE 7 The electrochemical impedance study with respect to TiO_2 wt.% variations in TiO_2-MWCNT nanocomposites. MWCNT, multiwalled carbon nanotube.

work can similarly be linked to the decreased ion transport caused by the location of TiO_2 active sites at or near the surface. As composites with higher wt.% of MWCNTs (lower TiO_2) had lower R_{CT}, the current study agreed with the report by Sundaram et al.[61] in that the MWCNT component plays a role in charge transfer reactions and internal resistance of the electrodes.

In the case of the 10 wt.% TiO_2 TiO_2-MWCNT composite, the absence of a semi-circle, and the presence of a straight line in the high-frequency region indicate a non-diffusion-controlled system and a relatively excellent capacitive behavior (Figure 7).[1,62] This agrees with the highest C_d value observed for the 10 wt.% TiO_2 nanocomposite (Table 3). Compared to pristine MWCNTs, the steeper and shorter curve of the 10 wt.% nanocomposites suggests a shorter diffusion pathlength that facilitates an improved capacitive character (Figure 7).

The equivalent series resistance (ESR), which is the sum of the electrode intrinsic resistance, electrolyte resistance, and contact resistance (current collector and material),[2,30] is the point of intersection of impedance and the Z_{re} axis (insert in Figure 7). The ESR variation was negligible since the aforementioned contributors were the same except for the TiO_2 wt.%. However, it was slightly lowered by an increase in TiO_2 wt.% (insert in Figure 7), and this corroborated with other TiO_2 composites synthesized by the sol-gel method.[2,14] Hence, the slight ESR variations can conceivably be regarded as negligible to the relative capacitive differences in the current composites.[30]

4 | CONCLUSIONS

The metal-organic chemical vapor deposition (MOCVD) of anatase TiO_2 on MWCNTs coated the tubes in bundled morphologies and successfully achieved the target TiO_2 loadings. Electrochemical characterization (CV, GCD analysis, and EIS) revealed that the 10 wt.% TiO_2 TiO_2-MWCNT nanocomposite exhibited the optimum capacitive behavior with associated E_s and P_s values of 55.56 and 2.78 W kg^{-1}, respectively, due to the synergism between the two components of the composite. In addition, C_s exhibited by the 20 wt.% TiO_2 TiO_2-MWCNT material was improved by more than 5000-fold from 5 wt.% TiO_2 at scan speeds of 100 and 200 mV s^{-1}. A higher TiO_2 wt.% induced fast charge/discharge capabilities, which facilitated high power density. The composition of the MOCVD synthesized composites influenced the associated physicochemical properties, such as the morphology and capacitive characteristics; hence, controlling the charge/discharge rates, pseudocapacitive contributions, and deliverable power density. The current study displayed that the MOCVD synthesis method imparts the TiO_2-MWCNT composites with suitable traits for improved EC applications.

ACKNOWLEDGMENTS

The authors acknowledge the University of KwaZulu-Natal (UKZN) and the UKZN Nanotechnology Platform for supporting this study by providing the necessary research infrastructure. This study is based on research supported wholly by the EPSRC Global Challenges Research Fund (GCRF) SUNRISE project (grant number: EP/P032591/1) and in part by the College of Agriculture, Engineering and Science, Eskom Tertiary Education Support Programme (TESP) and the National Research Foundation (NRF) of South Africa. MLD is grateful for the financial support of the EPSRC (EP/S001336/1) and grateful for the funding of the SPECIFIC Innovation and Knowledge Centre by the Engineering and Physical Science Research Council [EP/N020863/1], Innovate UK

[920036], and the European Regional Development Fund [c80892] through the Welsh Government.

CONFLICT OF INTEREST

The authors declare no conflict of interest.

ORCID

Edwin T. Mombeshora http://orcid.org/0000-0002-8333-9979
Bice S. Martincigh http://orcid.org/0000-0003-1426-5328

REFERENCES

1. Adhikari AD, Tiwari SK, Ha SK, Nayak GC. Boosted electrochemical performance of TiO_2 decorated RGO/CNT hybrid nanocomposite by UV irradiation. *Vacuum*. 2019;160:421-428. doi:10.1016/j.vacuum.2018.11.052
2. Elmouwahidi A, Bailón-García E, Castelo-Quibén J, Pérez-Cadenas AF, Maldonado-Hódar FJ, Carrasco-Marín F. Carbon–TiO_2 composites as high-performance supercapacitor electrodes synergistic effect between carbon and metal oxide phases. *J Mater Chem A*. 2018;6:633-644. doi:10.1039/C7TA08023A
3. Muchuweni E, Martincigh BS, Nyamori VO. Perovskite solar cells: current trends in graphene-based materials for transparent conductive electrodes, active layers, charge transport layers, and encapsulation layers. *Adv Energy Sustain Res*. 2021;2(9):2100050. doi:10.1002/aesr.202100050
4. Yasin MI, Khan MI, Alwadai N, Iqbal M. Facile synthesis of TiO_2 and Sn-TiO_2 heterostructures based photoanodes for dye sensitized solar cells. *Int J Energy Res*. 2021;45(13):18875-18884. doi:10.1002/er.6979
5. Wang Y, Zhang L, Hou H, et al. Recent progress in carbon-based materials for supercapacitor electrodes: a review. *J Mater Sci*. 2020;56:173-200. doi:10.1007/s10853-020-05157-6
6. Yang Y, Bremner S, Kay CMM. Battery energy storage system size determination in renewable energy systems: a review. *Renew Sustain Energy Rev*. 2018;91:109-125. doi:10.1016/j.rser.2018.03.047
7. Wang J, Lu K, Ma L, et al. Overview of compressed air energy storage and technology development. *Energies*. 2017;10(7):991-1013. doi:10.3390/en10070991
8. G SMM, Faraji F, Majazi A, Al-Haddad K. A comprehensive review of flywheel energy storage system technology. *Renew Sustain Energy Rev*. 2017;67:477-490. doi:10.1016/j.rser.2016.09.060
9. Jinyang F, Heping X, Jie C, et al. Preliminary feasibility analysis of a hybrid pumped-hydro energy storage system using abandoned coal mine goafs. *Appl Energy*. 2020;258:114007. doi:10.1016/j.apenergy.2019.114007
10. Nomoto S, Nakata H, Yoshioka K, Yoshida A, Yoneda H. Advanced capacitors and their applications. *J Power Sources*. 2001;97-98:807-811. doi:10.1016/S0378-7753(01)00612-7
11. Kang Z, Li Y, Yu Y, et al. Facile synthesis of $NiCo_2S_4$ nanowire arrays on 3D graphene foam for high-performance electrochemical capacitors application. *J Mater Sci*. 2018;53(14):10292-10301. doi:10.1007/s10853-018-2251-2
12. Chaudhary S, James LS, Kumar ABVK, et al. Reduced graphene oxide/ZnO nanorods nanocomposite: structural, electrical and electrochemical properties. *J Inorg Organomet Polym Mater*. 2019;29:2282-2290. doi:10.1007/s10904-019-01172-6
13. Hsieh C-T, Chen Y-C, Chen Y-F, Huq MM, Chen P-Y, Jan B-S. Microwave synthesis of titania-coated carbon nanotube composites for electrochemical capacitors. *J Power Sources*. 2014;269:526-533. doi:10.1016/j.jpowsour.2014.07.037
14. Hsieh C-T, Chen C-CCW-Y, Hung W-M. Electrochemical capacitance from carbon nanotubes decorated with titanium. *J Phys Chem Solids*. 2009;7:916-921. doi:10.1016/j.jpcs.2009.04.012
15. Allagui A, Freeborn TJ, Elwakil AS, Maundy BJ. Reevaluation of performance of electric double layer capacitors from constant-current charge/discharge and cyclic voltammetry. *Sci Rep*. 2017;6:38568. doi:10.1038/srep38568
16. Xu Y, Jiang J, Li Z, et al. Aerosol-assisted preparation of N-doped hierarchical porous carbon spheres cathodes toward high-stable lithium-ion capacitors. *J Mater Sci*. 2020;55(27):13127-13140. doi:10.1007/s10853-020-04955-2
17. Kampouris DK, Ji X, Randviir EP, Banks CE. A new approach for the improved interpretation of capacitance measurements for materials utilised in energy storage. *RSC Adv*. 2015;5:12782-12791. doi:10.1039/C4RA17132B
18. Eftekhari A, Li L, Yang Y. Polyaniline supercapacitors. *J Power Sources*. 2017;347:86-107. doi:10.1016/j.jpowsour.2017.02.054
19. Yi C-q, Zou J-p, Yang H-z, Leng X. Recent advances in pseudocapacitor electrode materials: transition metal oxides and nitrides. *Trans Nonferrous Met Soc China*. 2018;28:1980-2001. doi:10.1016/S1003-6326(18)64843-5
20. Daubert JS, Wang R, Ovental JS, et al. Intrinsic limitations of atomic layer deposition for pseudocapacitive metal oxides in porous electrochemical capacitor electrodes. *J Mater Chem A*. 2017;5:13086-13097. doi:10.1039/C7TA0279B
21. Fisher RA, Watt MR, Konjeti R, Read WJ. Atomic layer deposition of titanium oxide for pseudocapacitive functionalization of vertically-aligned carbon nanotube supercapacitor electrodes. *ECS J Solid State Sci Technol*. 2015;4(2):M1-M5. doi:10.1149/2.0141502jss
22. Mombeshora ET, Nyamori VO. A review on the use of carbon nanostructured materials in electrochemical capacitors. *Int J Energy Res*. 2015;39(15):1955-1980. doi:10.1002/er.3423
23. Kumar R, Singh BK, Soam A, Parida S, Sahajwalla V, Bhargava P. In situ carbon-supported titanium dioxide ($ICSTiO_2$) as an electrode material for high performance supercapacitors. *Nanoscale Adv*. 2020;2:2376-2386. doi:10.1039/D0NA00014K
24. Mugadza K, Stark A, Ndungu PG, Nyamori VO. Synthesis of carbon nanomaterials from biomass utilizing ionic liquids for potential application in solar energy conversion and storage. *Materials*. 2020;13:3945. doi:10.3390/ma13183945
25. Lu W, Qu L, Henry K, Dai L. High performance electrochemical capacitors from aligned carbon nanotube electrodes and ionic liquid electrolytes. *J Power Sources*. 2009;189(2):1270-1277. doi:10.1016/j.jpowsour.2009.01.009
26. Mombeshora ET, Ndungu PG, Jarvis ALL, Nyamori VO. Oxygen-modified multiwalled carbon nanotubes:

physicochemical properties and capacitor functionality. *Int J Energy Res*. 2017;41(8):1182-1201. doi:10.1002/er.3702
27. Mugadza K, Mombeshora ET, Stark A, Ndungu PG, Nyamori VO. Surface modifications of carbon nanotubes towards tailored electrochemical characteristics. *J Mater Sci Mater Electron*. 2021;32:27923-27936. doi:10.1007/s10854-021-07174-w
28. Jin F, Li M, Xie L, Jiang J. Selenium-doped carbon nanotubes/nickel selenide coaxial nanocables for energy storage. *J Power Sources*. 2021;514:230587. doi:10.1016/j.jpowsour.2021.230587
29. Kumar Y, Rawal S, Joshi B, Hashmi SA. Background, fundamental understanding and progress in electrochemical capacitors. *J Solid State Electrochem*. 2019;23(3):667-692. doi:10.1007/s10008-018-4160-3
30. Kim H-I, Kim H-J, Morita M, Park S-G. Preparation and electrochemical performance of CNT electrode with deposited titanium dioxide for electrochemical capacitor. *Bull Korean Chem Soc*. 2010;31(2):423-428. doi:10.5012/bkcs.2010.31.02.423
31. Almessiere MA, Slimani YA, Hassan M, Gondal MA, Cevik E, Baykal A. Investigation of hard/soft $CoFe_2O_4/NiSc_{0.03}Fe_{1.97}O_4$ nanocomposite for energy storage applications. *Int J Energy Res*. 2021;45(11):16691-16708. doi:10.1002/er.6916
32. Oseghe EO, Akpotu SO, Mombeshora ET, et al. Multidimensional applications of graphitic carbon nitride nanomaterials—a review. *J Mol Liq*. 2021;344:117820. doi:10.1016/j.molliq.2021.117820
33. Melchionna M, Prato M, Fornasiero P. Mix and match metal oxides and nanocarbons for new photocatalytic frontiers. *Catal Today*. 2016;277:202-213. doi:10.1016/j.cattod.2016.04.024
34. Mombeshora ET, Simoyi R, Nyamori VO, Ndungu PG. Multiwalled carbon nanotube-titania nanocomposites: understanding nano-structural parameters and functionality in dye-sensitized solar cells. *S Afr J Chem*. 2015;68:153-164. doi:10.17159/0379-4350/2015/v68a22
35. Beltram A, Melchionna M, Montini T, Nasi L, Fornasiero P, Prato M. Making H_2 from light and biomass-derived alcohols: the outstanding activity of newly designed hierarchical MWCNT/Pd@TiO_2 hybrid catalysts. *Green Chem*. 2017;19(10):2379-2389. doi:10.1039/c6gc01979j
36. Melchionna M, Beltram A, Stopin A, et al. Magnetic shepherding of nanocatalysts through hierarchically-assembled Fe-filled CNTs hybrids. *Appl Catal B*. 2018;227:356-365. doi:10.1016/j.apcatb.2018.01.049
37. Ray RS, Sarma B, Jurovitzki AL, Misra M. Fabrication and characterization of titania nanotube/cobalt sulfide supercapacitor electrode in various electrolytes. *Chem Eng J*. 2015;260:671-683. doi:10.1016/j.cej.2014.07.031
38. MamathaKumari M, Praveen Kumar D, Haridoss P, DurgaKumari V, Shankar MV. Nanohybrid of titania/carbon nanotubes—nanohorns: a promising photocatalyst for enhanced hydrogen production under solar irradiation. *Int J Hydrogen Energy*. 2015;40(4):1665-1674. doi:10.1016/j.ijhydene.2014.11.117
39. Tan W, Gao T, Wang Y. Influence of surface potential on the capacitive performance of the TiO_2 thin-film electrode with different crystalline forms. *Langmuir*. 2020;36(14):3836-3842. doi:10.1021/acs.langmuir.0c00663
40. Salari M, Aboutalebi SH, Chidembo AT, Nevirkovets IP, Konstantinov K, Liu HK. Enhancement of the electrochemical capacitance of TiO_2 nanotube arrays through controlled phase transformation of anatase to rutile. *Phys Chem Chem Phys*. 2012;14(14):4770-4779. doi:10.1039/c2cp40410a
41. Manickam M, Singh P, Issa TB, Thurgate S. Electrochemical behavior of anatase TiO_2 in aqueous lithium hydroxide electrolyte. *J Appl Electrochem*. 2006;36(5):599-602. doi:10.1007/s10800-005-9112-9
42. Krishnaveni M, Anandan AMAS. Ultrasound-assisted synthesis of unzipped multiwalled carbon nanotubes/titanium dioxide nanocomposite as a promising next-generation energy storage material. *Ultrasonics Sonochemistry*. 2020;66:105105. doi:10.1016/j.ultsonch.2020.105105
43. Mombeshora ET, Nyamori VO. Physicochemical characterisation of graphene oxide and reduced graphene oxide composites for electrochemical capacitors. *J Mater Sci Mater Electron*. 2017;28(24):18715-18734. doi:10.1007/s10854-017-7821-6
44. Berki P, Reti B, Terzi K, et al. The effect of titania precursor on the morphology of prepared TiO_2/MWCNT nanocomposite materials. *Phys Status Solidi B*. 2014;251(12):2384-2388. doi:10.1002/pssb.201451161
45. Qian L, Du Z-L, Yang S-Y, Jin Z-S. Raman study of titania nanotube by soft chemical process. *J Mol Struct*. 2005;749:103-107. doi:10.1016/j.molstruc.2005.04.002
46. Hardcastle FD, Ishihara H, Sharma R, Biris AS. Photoelectroactivity and Raman spectroscopy of anodized titania (TiO_2) photoactive water-splitting catalysts as a function of oxygen-annealing temperature. *J Mater Chem*. 2011;21(17):6337-6345. doi:10.1039/c0jm03106b
47. Paul S, Choudhury A. Investigation of the optical property and photocatalytic activity of mixed phase nanocrystalline titania. *Appl Nanosci*. 2014;4(7):839-847. doi:10.1007/s13204-013-0264-3
48. Li X, Niu J, Zhang J, Li H, Liu Z. Labeling the defects of single-walled carbon nanotubes using titanium dioxide nanoparticles. *J Phys Chem B*. 2003;107(11):2453-2458. doi:10.1021/jp026887y
49. Georgios P, Wolfgang SM. X-ray photoelectron spectroscopy of anatase-TiO_2 coated carbon nanotubes. *Solid State Phenom*. 2010;162:163-177. doi:10.4028/www.scientific.net/SSP.162.163
50. Li Y, Li L, Li C, Chen W, Zeng M. Carbon nanotube/titania composites prepared by a micro-emulsion method exhibiting improved photocatalytic activity. *Appl Catal A*. 2012;427:1-7. doi:10.1016/j.apcata.2012.03.004
51. Yu Y, Yu JC, Chan C-Y, et al. Enhancement of adsorption and photocatalytic activity of TiO_2 by using carbon nanotubes for the treatment of azo dye. *Appl Catal B*. 2005;61(1-2):1-11. doi:10.1016/j.apcatb.2005.03.008
52. Qing R, Liu L, Kim H, Sigmund WM. Electronic property dependence of electrochemical performance for TiO_2/CNT core-shell nanofibers in lithium ion batteries. *Electrochim Acta*. 2015;180:295-306. doi:10.1016/j.electacta.2015.08.097
53. Biswal A, Panda PK, Acharya AN, et al. Tuning the morphology and redox behaviour by varying the concentration of Fe in a CoNiFe ternary oxide heterostructure for hybrid devices. *New J Chem*. 2020;44(23):9921-9932. doi:10.1039/d0nj01486a

54. Elgrishi Nm, Rountree KJ, McCarthy BD, Rountree ES, Eisenhart TT, Dempsey JL. A practical beginner's guide to cyclic voltammetry. *J Chem Educ*. 2018;95:197-206. doi:10.1021/acs.jchemed.7b00361
55. Ji H, Zhao X, Qiao Z, et al. Capacitance of carbon-based electrical double-layer capacitors. *Nat Commun*. 2014;5:3317. doi:10.1038/ncomms4317
56. Rashti A, Lu X, Dobson A, et al. Tuning MOF-derived Co_3O_4/$NiCo_2O_4$ nanostructures for high-performance energy storage. *ACS Appl Energy Mater*. 2021;4(2):1537-1547. doi:10.1021/acsaem.0c02736
57. Choi C, Ashby DS, Butts DM, et al. Achieving high energy density and high power density with pseudocapacitive materials. *Nat Rev Mater*. 2019;5(1):5-19. doi:10.1038/s41578-019-0142-z
58. Portet C, Taberna PL, Simon P, Flahaut E, Laberty-Robert C. High power density electrodes for carbon supercapacitor applications. *Electrochim Acta*. 2005;50(20):4174-4181. doi:10.1016/j.electacta.2005.01.038
59. Wang Y, Song Y, Xia Y. Electrochemical capacitors: mechanism, materials, systems, characterization and applications. *Chem Soc Rev*. 2016;45(21):5925-5950. doi:10.1039/c5cs00580a
60. Ahn YR, Park CR, Jo SM, Kim DY. Enhanced charge-discharge characteristics of RuO_2 supercapacitors on heat-treated TiO_2 nanorods. *Appl Phys Lett*. 2007;90(12):122106. doi:10.1063/1.2715038
61. Sundaram MM, Appadoo D. Traditional salt-in-water electrolyte vs. water-in-salt electrolyte with binary metal oxide for symmetric supercapacitors: capacitive vs. faradaic. *Dalton Trans*. 2020;49(33):11743-11755. doi:10.1039/d0dt01871f
62. Mombeshora ET, Ndungu PG, Jarvis ALL, Nyamori VO. The physical and electrochemical properties of nitrogen-doped carbon nanotube- and reduced graphene oxide-titania nanocomposites. *Mater Chem Phys*. 2018;213:102-112. doi:10.1016/j.matchemphys.2018.03.076

SUPPORTING INFORMATION

Additional supporting information can be found online in the Supporting Information section at the end of this article.

How to cite this article: Mombeshora ET, Muchuweni E, Davies ML, Nyamori VO, Martincigh BS. Metal-organic chemical vapour deposition of anatase titania on multiwalled carbon nanotubes for electrochemical capacitors. *Energy Sci. Eng*. 2022;1-14. doi:10.1002/ese3.1234